Brain Structure and Function (2019) 224:2103–2119
https://doi.org/10.1007/s00429-019-01896-8

ORIGINAL ARTICLE

Thyroid hormone availability in the human fetal brain: novel entry pathways and role of radial glia

Daniela López-Espíndola[1,2] · Ángel García-Aldea[1] · Inés Gómez de la Riva[4] · Ana Margarita Rodríguez-García[4] · Domenico Salvatore[6,7] · Theo J. Visser[5] · Juan Bernal[1,3] · Ana Guadaño-Ferraz[1,3]

Received: 8 January 2019 / Accepted: 27 May 2019 / Published online: 4 June 2019

Abstract

Thyroid hormones (TH) are crucial for brain development; their deficiency during neurodevelopment impairs neural cell differentiation and causes irreversible neurological alterations. Understanding TH action, and in particular the mechanisms regulating TH availability in the prenatal human brain is essential to design therapeutic strategies for neurological diseases due to impaired TH signaling during neurodevelopment. We aimed at the identification of cells involved in the regulation of TH availability in the human brain at fetal stages. To this end, we studied the distribution of the TH transporters monocarboxylate transporter 8 (MCT8) and organic anion-transporting polypeptide 1C1 (OATP1C1), as well as the TH-metabolizing enzymes types 2 and 3 deiodinases (DIO2 and DIO3). Paraffin-embedded human brain sections obtained from necropsies of thirteen fetuses from 14 to 38 gestational weeks were analyzed by immunohistochemistry and in situ hybridization. We found these proteins localized along radial glial cells, in brain barriers, in Cajal-Retzius cells, in migrating fibers of the brainstem and in some neurons and glial cells with particular and complex spatiotemporal patterns. Our findings point to an important role of radial glia in controlling TH delivery and metabolism and suggest two additional novel pathways for TH availability in the prenatal human brain: the outer, and the inner cerebrospinal fluid–brain barriers. Based on our data we propose a model of TH availability for neural cells in the human prenatal brain in which several cell types have the ability to autonomously control the required TH content.

Keywords Thyroid hormones · Human fetal brain · Thyroid hormone transporters · Deiodinases · Brain barriers · Radial glial cells

Introduction

Thyroid hormones (TH), T4 (3,5,3′,5′-tetraiodo-L-thyronine or thyroxine), and T3 (3,5,3′-triiodo-L-thyronine) are crucial for brain development and function. TH action is

Electronic supplementary material The online version of this article (https://doi.org/10.1007/s00429-019-01896-8) contains supplementary material, which is available to authorized users.

✉ Juan Bernal
jbernal@iib.uam.es

✉ Ana Guadaño-Ferraz
aguadano@iib.uam.es

1 Department of Endocrine and Nervous System Pathophysiology, Instituto de Investigaciones Biomédicas Alberto Sols, Consejo Superior de Investigaciones Científicas (CSIC), Universidad Autónoma de Madrid (UAM), 28029 Madrid, Spain

2 Escuela de Tecnología Médica and Centro de Investigaciones Biomédicas (CIB), Universidad de Valparaíso, Angamos 655, Reñaca, Viña del Mar, Chile

3 Center for Biomedical Research on Rare Diseases (CIBERER), U708, Madrid, Spain

4 Pathology Department, La Paz University Hospital, 28046 Madrid, Spain

5 Department of Internal Medicine, Erasmus Medical Center, 3015 GD Rotterdam, The Netherlands

6 Department of Public Health, University of Naples "Federico II", 80133 Naples, Italy

7 CEINGE-Biotecnologie Avanzate s.c.a.r.l, 80145 Naples, Italy

exerted mainly by the interaction of the active hormone T3 with nuclear receptors and regulation of gene expression. Studies in experimental animals indicate that TH control neuronal migration, cortical lamination, cortical circuitry formation, differentiation of neural cells, and myelination. In humans, TH availability and action at critical prenatal stages may result in permanent and irreversible brain damage unless adequate treatment is undertaken. Adverse conditions include maternal hypothyroxinemia and hypothyroidism during pregnancy, congenital hypothyroidism, endemic cretinism, and mutations in T3 receptors, and in the gene encoding the TH-specific transporter monocarboxylate transporter 8 (MCT8) (DeLong 1993; Bernal 2007; Morreale de Escobar et al. 2004; Dumitrescu and Refetoff 2013; López-Espíndola et al. 2014; Dumitrescu et al. 2004; Friesema et al. 2004; Bernal et al. 2015).

The supply of TH for neural cells is regulated by TH transporters and deiodinases. The transporters are integral membrane proteins that mediate the cellular influx and efflux of TH. Studies in postnatal rodents have shown that TH require transporters to cross the blood–brain barrier (BBB) (Bernal et al. 2015), and to a lesser extent, the blood–cerebrospinal fluid barrier (BCSFB) (Dratman et al. 1991). In the fetal brain there are two additional barriers, the outer and the inner cerebrospinal fluid–brain barriers (CSFBB) (Saunders et al. 2018). The outer CSFBB, formed by intercellular junctions between pial leptomeningeal cells and the basal end-feet of radial glial cells (RG) (Brochner et al. 2015), restricts the passage of molecules from the CSF in the subarachnoid space to the cerebral cortex. The inner CSFBB, disappearing later in development, is formed by strap junctions present in the neuroepithelial cells lining the ventricular system that differentiate subsequently into RG. This barrier restricts the exchange of substances between the CSF and the ventricular zone (VZ) (Mollgard and Saunders 1986; Whish et al. 2015). It is unknown at present whether brain TH availability is regulated by these barriers.

Experimental and clinical data point to MCT8 and the organic anion transporter polypeptide 1C1 (OATP1C1) as the major TH transporters in the brain (Dumitrescu et al. 2004; Friesema et al. 2004; Ceballos et al. 2009; Mayerl et al. 2014; Vatine et al. 2017). MCT8 is a highly specific transporter for T4 and T3, and other TH derivatives (Friesema et al. 2003). OATP1C1 transports T4 and steroid hormone metabolites (Westholm et al. 2009) and does not transport T3. Previous studies have reported the presence of MCT8 and OATP1C1 in the BBB and the BCSFB in the fetal and adult human brain. MCT8 is abundant in both barriers and OATP1C1 is high in the BCSFB but very low in the BBB (Wirth et al. 2009; Chan et al. 2011, 2014; Roberts et al. 2008; Friesema et al. 2012). MCT8 and OATP1C1 have also been localized in ependymal cells, tanycytes and neurons (Friesema et al. 2012; Wirth et al. 2009; Chan et al. 2014; Alkemade et al. 2005, 2011). MCT8 has also been detected in cells of the VZ and subventricular (SVZ) zones (Chan et al. 2014; Kallo et al. 2012).

The cellular availability of TH in the brain is also controlled by the deiodinase enzymes types 2 (DIO2) and 3 (DIO3). DIO2 is an activating enzyme, generating T3 by outer ring deiodination of T4. DIO3 inactivates T4 and T3 through inner ring deiodination, producing rT3 (3,3′,5′-triiodo-L-thyronine) from T4 and 3,3′-T2 from T3 (Gereben et al. 2008). In humans, DIO2 and DIO3 localization has been studied in the developing and adult hypothalamus. DIO2 is localized surrounding blood vessels, and in the choroid plexus, tanycytes, and astrocytes, and DIO3 in the choroid plexus, and in hypothalamic neurons and axons (Friesema et al. 2012; Alkemade et al. 2005; Kallo et al. 2012). Brain T3 is derived in part from the circulation, and in part from local T4 deiodination in astrocytes (Guadaño-Ferraz et al. 1997). In the fetus, most if not all brain T3 is formed locally from T4 (Calvo et al. 1990; Grijota-Martínez et al. 2011; Kester et al. 2004). As development proceeds during postnatal stages the proportion of T3 derived from the circulation increases, reaching around 50% of total brain T3 (Crantz et al. 1982; Galton et al. 2007; Dumitrescu et al. 2006; Trajkovic et al. 2007; Morreale de Escobar et al. 2004; Larsen et al. 1981). The current model of TH delivery to the brain in rodents predicts that circulating T4 crosses the BBB through MCT8 and OATP1C1 and is converted to T3 in astrocytes (Morte and Bernal 2014; Bernal et al. 2015). MCT8 is the main transporter for T3 but despite its presence in the rodent fetal brain circulating T3 does not reach this organ for unknown reasons (Grijota-Martínez et al. 2011). The brain pool of T3 is, therefore, entirely dependent on local production, and once formed, T3 would be available to neural cells possibly through diverse membrane transporters (Bernal et al. 2015). It is unknown whether this model applies to humans. This is partially due to the limited knowledge on the cellular distribution of transporters and deiodinases in the human fetal brain. Indeed, fundamental differences must exist between humans and rodents since MCT8 deficiency in mice minimally affects the nervous system in sharp contrast to patients with *MCT8/SLC16A2* mutations (Wirth et al. 2009). One possible explanation is the higher abundance of OATP1C1 in the mouse BBB, compared to humans and monkeys, permitting T4 uptake and conversion to T3 in the absence of MCT8 (Roberts et al. 2008; Morte and Bernal 2014; Ito et al. 2011).

The present work aims at a better understanding of the entry pathways and the mechanisms regulating TH availability during human prenatal neurodevelopment. To this end, we have performed an extensive analysis of the regional and cellular expression of MCT8, OATP1C1, DIO2, and DIO3 in several human fetal brain regions at different gestational ages, using immunohistochemistry and in situ hybridization

techniques. We show that transporters and deiodinases display a complex expression pattern in the human fetal brain. We propose a model that includes two novel entry pathways for TH in the brain located in the cerebrospinal fluid–brain interface. Our results also suggest, for the first time, a key role for RG in the availability of TH during cerebral cortex development, and in the generation of the active hormone T3. We believe that these findings are relevant to therapeutic approaches for neurological diseases with an origin in TH imbalances at prenatal stages.

Materials and methods

Subjects and brain tissue

Paraffin blocks of brain tissue from 12 fetuses at gestational weeks (GW) 14, 16, 20, 25, 30, 32, and 38 without known brain pathology were provided by the IdiPAZ Biobank. The samples included frontal, parietal, temporal and occipital cortex, intermediate zone (IZ), SVZ, VZ, ventricular epithelium, hippocampal formation, brainstem, choroid plexus, and meninges. Blocks from a GW30 MCT8-deficient fetus (*MCT8* mutation L494P) were provided by the Wolfson Medical Center, Holon, Israel, and the Sackler School of Medicine, Tel Aviv, Israel with written informed consent from the parents (Online Supplementary Resource 1). All procedures followed the 1964 Helsinki Declaration and were approved by the ethics committee of our Institution (Consejo Superior de Investigaciones Científicas, permit number SAF2011-2560). The smallest possible number of samples was used to perform these studies and personal data were treated anonymously.

Tissue processing

Upon collection, the tissue samples were fixed in 4% formaldehyde for 15 days, then postfixed in Bouin's solution for 6 h and embedded in paraffin using standard procedures. Seven micrometer thin sections were examined histologically by hematoxylin–eosin staining (HT110332, HHS32, Sigma-Aldrich, Darmstadt, Germany) following standard protocols, and also by immunohistochemistry (IHC), immunofluorescence (IF), and in situ hybridization.

Immunohistochemistry

Three MCT8 antibodies were used: a rabbit polyclonal anti-MCT8 AB_611613 (IHC 1:700/IF 1:200, HPA003353 Atlas Antibodies, Bromma, Sweden) (Wirth et al. 2011); a rabbit polyclonal anti-MCT8 hMCT81306 (IHC 1:100/IF 1:50) (Alkemade et al. 2005) and a rabbit polyclonal anti-MCT8 XE045 (IHC 1:100, kindly donated by Roberts 2008). For OATP1C1 we used two antibodies: a rabbit polyclonal anti-OATP1C1 hOATP1C13516 (IHC 1:500/IF 1:100) (Alkemade et al. 2011) and a rabbit polyclonal anti-OATP1C1 XE066 (IHC 1:200/IF 1:50, kindly donated by Roberts 2008). The DIO2 antibody was the rabbit polyclonal AB_2261556 (IHC 1:100/IF 1:50, sc-98716 Santa Cruz Biotechnology, Dallas, TX, USA) (Yamaguchi et al. 2012). The DIO3 antibody was the rabbit polyclonal abD3-718 (IHC 1:700/IF 1:200) (Huang et al. 2002; Howard et al. 2011). We also used the following antibodies listed in the JCN Antibody Database and registered in the Antibody Registry (http://antibodyregistry.org/): mouse monoclonal anti-GFAP AB_477010 (IHC 1:200/IF 1:50, G3893, clone G-A-5, Sigma-Aldrich, Darmstadt, Germany); mouse monoclonal anti-vimentin AB_10013485 (IHC 1:200/IF 1:50, M0725, clone V9, Dako, Santa Clara, CA, USA); mouse monoclonal anti-nestin AB_2251134 (IHC 1:200/IF 1:50, MAB5326, clone 10C2, Millipore, Darmstadt, Germany); mouse monoclonal anti-reelin AB_2179313 (1:200, MAB5364, clone G10, Millipore, Darmstadt, Germany) and goat polyclonal anti-Olig2 AB_2157554 (1:30, RYD-AF2418, R&D Systems, Minneapolis, MN, USA). As secondary antibodies, we used goat anti-rabbit biotinylated and horse anti-mouse biotinylated (1:200, BA-1000, BA-2000, Vector Laboratories, Burlingame, CA, USA) and goat anti-rabbit IgG AF488 and goat anti-mouse IgG AF546 (1:500; A11034, A11030 Molecular Probes, Waltham, MA, USA).

Immunohistochemical procedures were performed as previously described (López-Espíndola et al. 2014). For immunofluorescence, tissues were incubated with Alexafluor®-conjugated secondary antibodies, DAPI counterstained (D1306, Molecular Probes, Waltham, MA, USA), and coverslipped with Prolong (P36930, Molecular Probes, Waltham, MA, USA). To avoid methodological differences, samples from the same brain regions at different developmental stages were processed simultaneously for every antibody and with a negative control without the primary antibody (Online Supplementary Resource 2). Whenever possible, to obtain more reliable results, the same protein was analyzed with different antibodies against different epitopes. The different antibodies for MCT8 and for OATP1C1 gave similar immunostaining patterns. The almost absence of MCT8 immunoreactivity in the MCT8-deficient fetus confirms the specificity of the MCT8 antibodies (Online Supplementary Resource 3). The immunoreactive staining patterns are qualitatively described as weak, moderate or strong, compared to its maximum signal observed in all regions and ages studied.

Radioactive in situ hybridization

Radioactive in situ hybridization combined with nestin immunohistochemistry or counterstained with hematoxylin

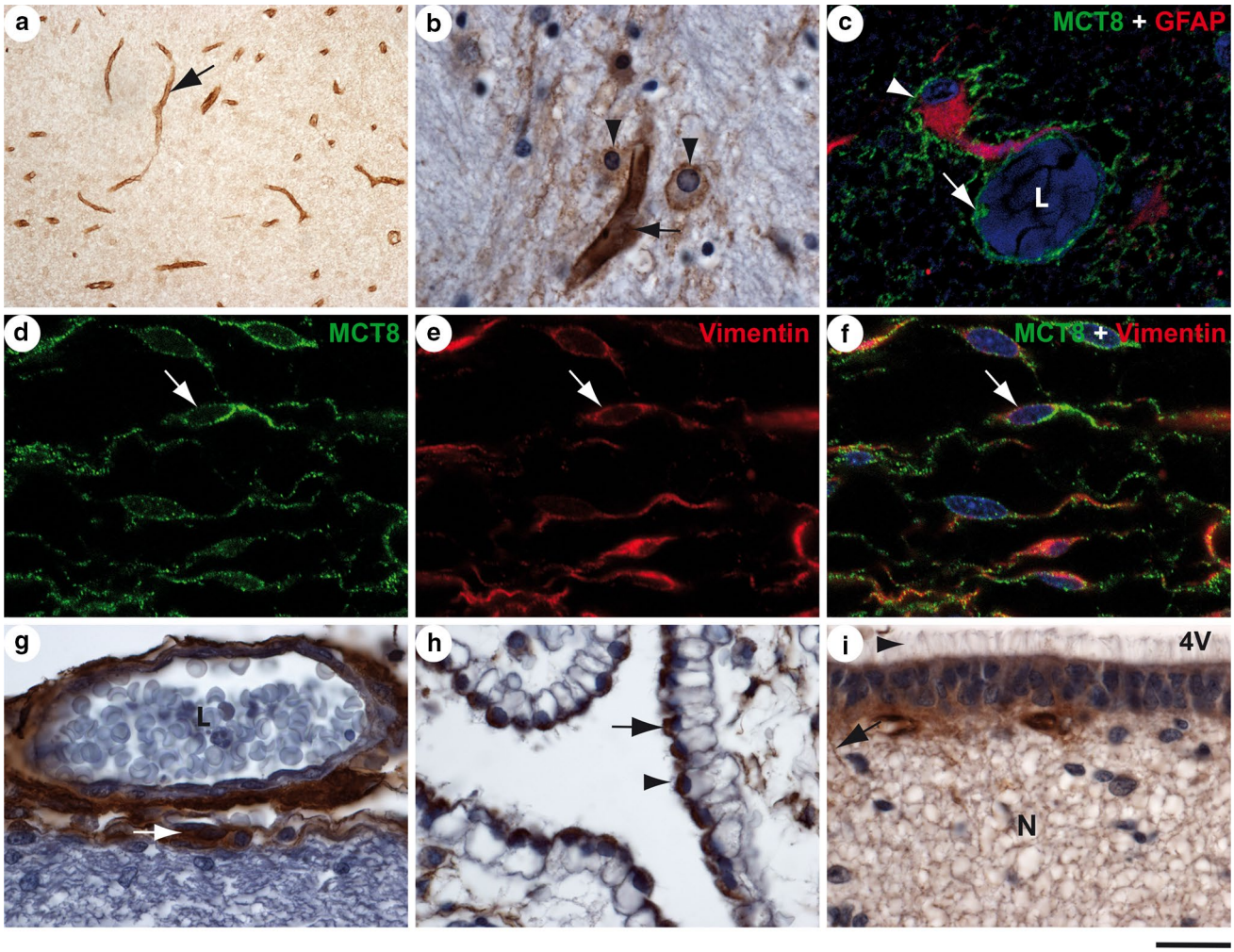

Fig. 1 MCT8 immunostaining in the fetal cerebral barriers. Representative photomicrographs showing immunohistochemical (brown color) and immunofluorescence (green color) staining of MCT8 in the BBB (**a**–**c**), the meninges and the outer cerebrospinal fluid-brain barrier (**d**–**g**), the blood–cerebrospinal fluid barrier (**h**) and the epithelium of the fourth ventricle (**i**) in control fetuses at GW16 (**d**–**h**), GW25 (**a**, **i**) and GW32 (**b**, **c**). Tissue sections were also counterstained with hematoxylin or DAPI (blue color). Arrows in **a**–**c** show MCT8 immunostaining associated with blood vessels comprising the BBB. Arrowheads in **b** and **c** point to glial cells surrounding blood vessels identified as astrocytes immunopositive for GFAP in immunofluorescence assays (**c**, GFAP in red). Arrows in **d**–**g** point to MCT8 immunoreactivity in leptomeningeal cells identified as vimentin immunopositive cells (**e**, **f**, vimentin in red) comprising the outer cerebrospinal fluid-brain barrier. Note in **g** the strong MCT8 immunoreactivity in the subarachnoid blood vessels. Arrow in **h** points to MCT8 immunostaining in the apical portion of choroid plexus epithelial cells comprising the blood-cerebrospinal fluid barrier, while arrowhead points to MCT8 immunostaining in the epithelial cells' cilia. In **i** MCT8 immunostaining is present in the ependymocytes, both in the cytoplasm and cilia (arrowhead) and in their basal processes (arrow) running across the subventricular neuropil. *L* blood vessel lumen, 4 *V* fourth ventricle, *N* neuropil. Scale bar represents 115 µm (**a**); 23 µm (**b**, **g**–**i**) and 12 µm (**c**, **d**–**f**)

was performed as previously described (Bernal and Guadaño-Ferraz 2002) with the required modifications for paraffin tissue sections. Tissue sections were deparaffinized in xylene, hydrated and processed in 0.30 M sodium citrate and 0.03 M NaCl buffer for auto-crosslinking at 1200 µJ. The riboprobe cDNA templates were obtained by PCR using total RNA from human fetal brain (636,526, Clontech Laboratories, Takara Bio, Kusatsu, Shiga, Japan) and subcloned in pGEM®-T Easy (A1360, Promega, Wisconsin, USA). The specific oligonucleotide pairs used were: *MCT8*: 5′-ATC TGGGCCTTCGGAATTGC-3′, 5′-GGTAGCCAATGG CCTGTGAG-3′; *OATP1C1*: 5′-AGGCATAGTGGGAAG ATGTC-3′, 5′-TGGGATGCTGTAGCAATGAG-3′; *DIO2*: 5′-AGAGTTCTCCTCAGTGGCTG-3′, 5′-TCAGTAAGC CAATAGGGCTC-3′ and *DIO3*: 5′-AGAGCCAGCACATCC TCGAC-3′, 5′-CGCAGCTCAGAGACCTGGTA-3′. Sense and antisense probes were transcribed with RNA polymerase enzymes (Roche Molecular Biochemicals, Mannheim,

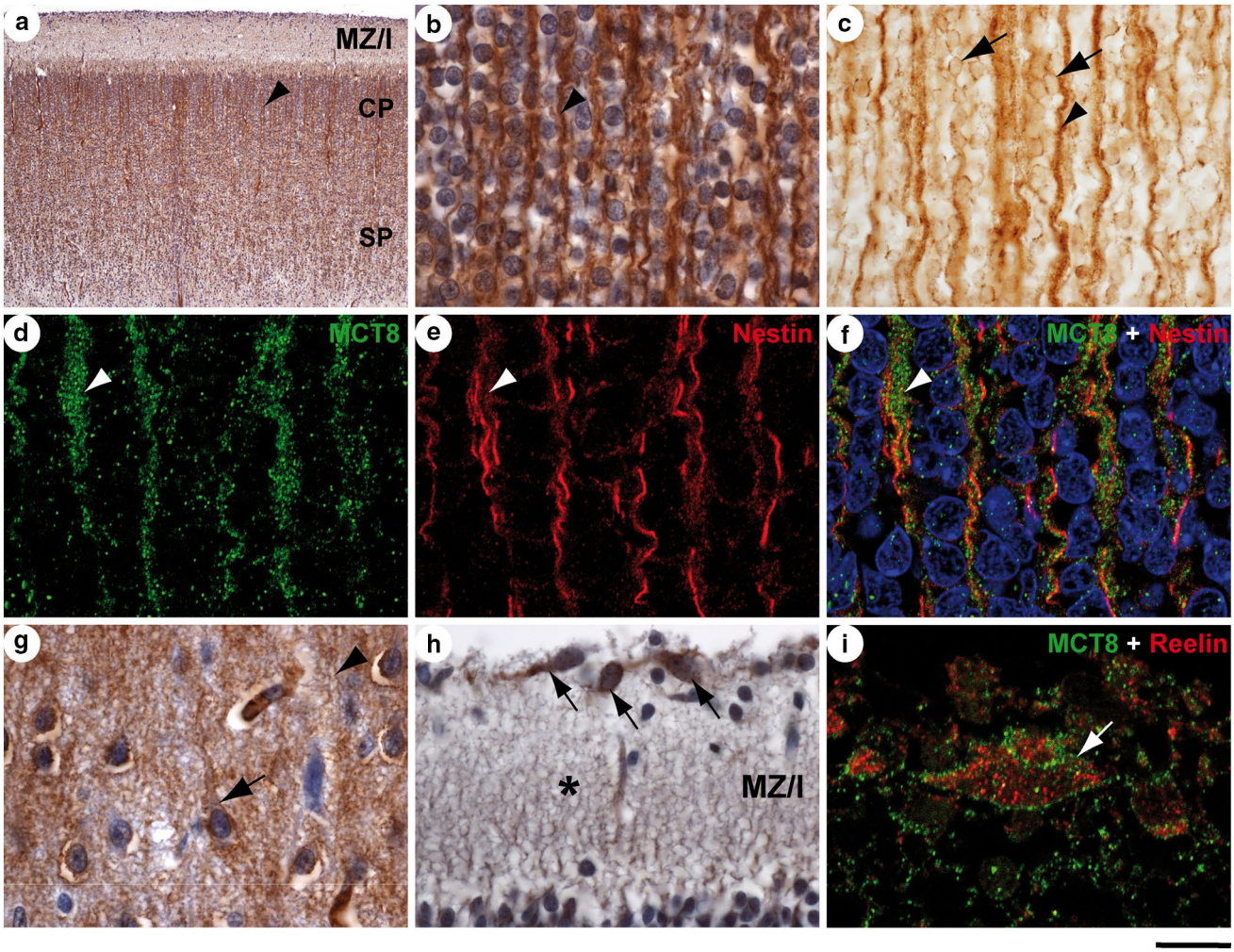

Fig. 2 MCT8 immunostaining in the fetal cerebral cortex. Representative photomicrographs showing immunohistochemical (brown color) and immunofluorescence (green color) staining of MCT8 in the cerebral cortex of control fetuses at GW14 (**d**–**f**, **h**), GW16 (**i**), GW20 (**a**–**c**) and GW38 (**g**). Tissue sections were also counterstained with hematoxylin or DAPI (blue color). Arrowheads in **a**–**g** point to the strong MCT8 immunoreactivity detected in RG basal processes, which are also immunopositive for nestin (**e**, **f**, nestin in red). Arrows in **c** and **g** point to MCT8 immunoreactivity at the cellular membrane of cortical plate neurons. Arrows in **h** and **i** point to MCT8 immunopositive Cajal–Retzius cells, which were characterized as immunopositive for reelin (**i**, reelin in red). Asterisk in h point to immunopositive endfeet of RG basal processes in MZ/I. *CP* cortical plate, *SP* Subplate, *MZ/I* Marginal zone/layer I. Scale bar represents 230 µm (**a**); 23 µm (**b**, **c**, **g**, **h**) and 12 µm (**d**–**f**, **i**)

Germany) in the presence of ^{35}S-UTP (NEG039H, PerkinElmer, Waltham, MA, USA), and purified in Chromaspin 100 columns (Clontech Laboratories, Takara Bio, Kusatsu, Shiga, Japan). Exposure time after hybridization was 60–90 days. The thin thickness of the sections limited the sensitivity of the procedure and only cells with a high content of *MCT8* mRNA could be detected.

Tissue analysis

Tissue slices were analyzed on an Eclipse E400 light microscope. Images were captured with a digital camera (Dn100, Nikon, Tokyo, Japan) and NIS software (Nikon, Tokyo, Japan). Immunofluorescence was analyzed on a confocal microscope (LSM 710 Spectral Confocal Microscope, Zeiss, Oberkochen, Germany). Images were acquired with the ZEN 2009 software and processed with the ZEN 2012 program (Zeiss, Oberkochen, Germany). Adobe Illustrator and Adobe Photoshop CS4 (Adobe Systems, CA, USA) were used to create the artwork.

The "Atlas of human central nervous system development" (Bayer and Altman 2003, 2005) was used for histological analyses and nomenclature of brain structures and regions.

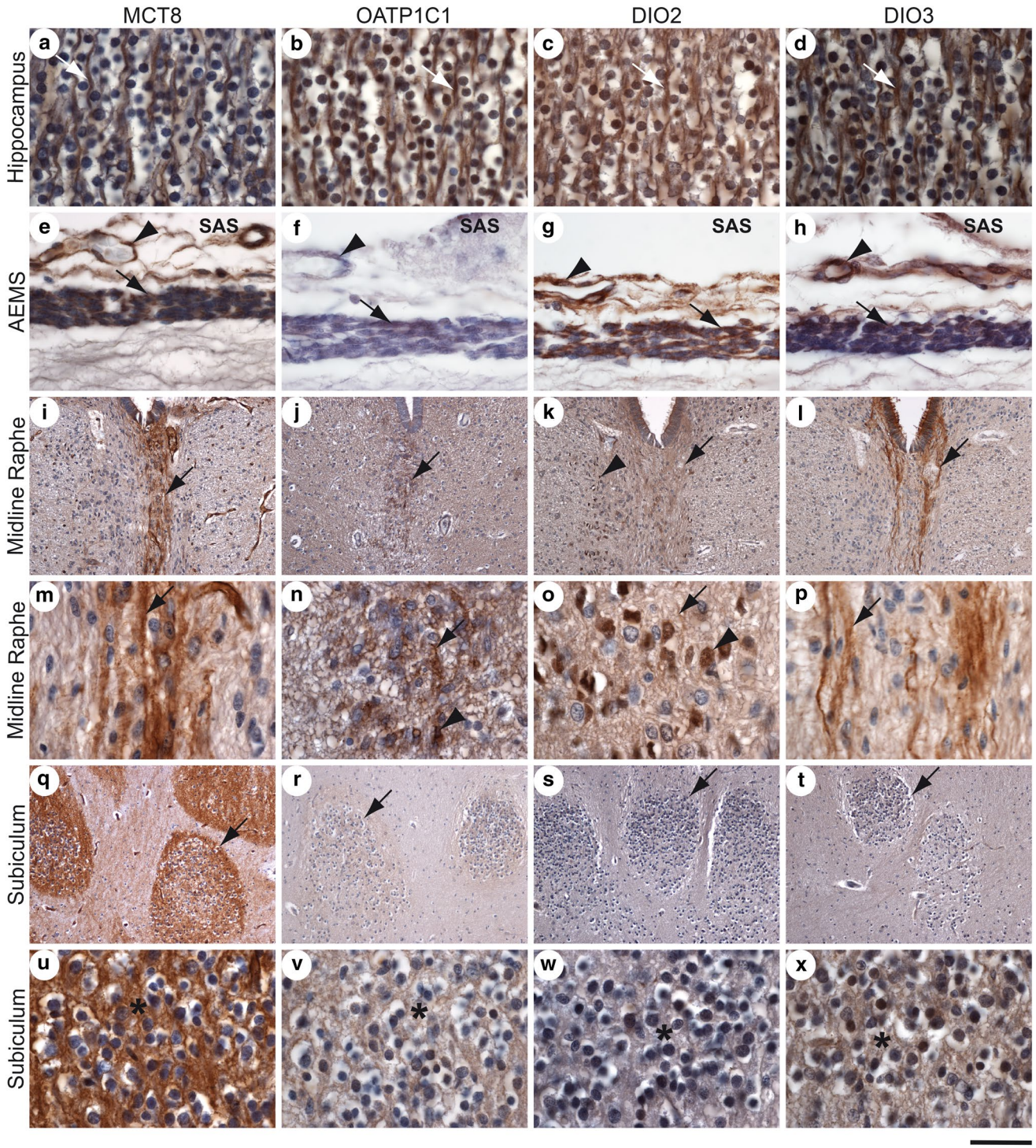

Analysis of single cell transcriptomics database

Pollen et al. (2015) have recently performed transcriptomic analysis of single RG micro dissected from GW16-18 human fetal cortex. Using their published database we searched for single cell expression of *SLCO1C1* and *SLC16A2*, other secondary thyroid hormone transporters (Bernal et al. 2015), *DIO2,* thyroid hormone receptors *THRA* and *THRB*, and a glia (*VIM*) or neuronal marker (*SSTR2*). The data were extracted from the mmc3 file published as supplementary information (Pollen et al. 2015). This file contains transcriptomic data on 393 isolated cells, 188 from the VZ, and 205 from the SVZ. Coexpression of different mRNAs in the

◂**Fig. 3** MCT8, OATP1C1, DIO2, and DIO3 immunostaining in cellular migratory routes in the fetal brain. Representative photomicrographs showing MCT8 (**a**, **e**, **i**, **m**, **q**, **u**), OATP1C1 (**b**, **f**, **j**, **n**, **r**, **v**), DIO2 (**c**, **g**, **k**, **o**, **s**, **w**) and DIO3 (**d**, **h**, **l**, **p**, **t**, **x**) immunostaining (brown color) in RG basal processes in the cornus ammonis of the hippocampus (**a**–**d**), in fibers from the anterior extramural migratory stream (AEMS; **e**–**h**), in the midline raphe glial fibers (**i**–**p**) and in nests of migrating granule cells in the subiculum (**q**–**x**), in control fetuses at GW14 (**e**–**h**), GW16 (**a**–**d**), GW20 (**l**, **p**) and GW25 (**i**–**k**, **m**–**o**, **q**–**x**). Tissue sections were also counterstained with hematoxylin staining (blue color). Arrows in **a**–**p** indicate localization of transporters and deiodinases in migrating fibers. Note in the hippocampus (**a**–**d**) the strong immunoreactivity for all the proteins in RG basal processes. Arrowheads in **e**–**h** indicate the localization of transporters and deiodinases associated to blood vessels. Note in **f** the weak OATP1C1 immunoreactivity in AEMS fibers and blood vessels. Images in **m**–**p** correspond to amplifications of **i**–**l**, respectively. Note the strong MCT8 and DIO3 immunoreactivity in the midline raphe glial fibers (**i**, **l**, **m**, **p**). Arrowheads in **k**, **n** and **o** point to OATP1C1 and DIO2 immunopositive cells of the raphe nuclear complex. Arrows in **q**–**t** point to nest of granule cells in the subiculum. Images in **u**–**x** correspond to amplifications of **q**–**t**, respectively. Asterisks in **u**–**x** point to the immunopositive neuropil of the nests of granule cells. Note the strong MCT8 immunostaining in **q** and **u**. *SAS* Subarachnoid space. Scale bar represents 31 µm (**a**–**h**, **m**–**p**, **u**–**x**) and 154 µm (**i**–**l**, **q**–**t**)

same cells was analyzed using Venny software (Oliveros 2007–2015).

Results

We analyzed the expression of TH transporters and deiodinases in different brain regions of human fetuses from GW14 to GW38 as detailed in the supplementary information (MCT8 in Online Supplementary Resource 4; OATP1C1 in Online Supplementary Resource 5; DIO2 in Online Supplementary Resource 6 and DIO3 in Online Supplementary Resource 7). Figures in this section show the most representative results.

MCT8 is present in the brain barriers and ventricular system

From the first age studied (GW14) onwards, strong MCT8 immunoreactivity was associated with blood vessels in all brain regions (Fig. 1a–c, Online Supplementary Resources 3a, c, and 4). An interesting finding was the presence of moderate MCT8 levels in GFAP-immunopositive cells surrounding parenchymal blood vessels at GW32 and 38 (Fig. 1b, c, and Online Supplementary Resource 4). At all ages, MCT8 exhibited strong immunoreactivity in the leptomeninges, specifically in the membrane of vimentin-immunopositive cells present in the arachnoid and pia mater (Fig. 1d–g and Online Supplementary Resource 4). In the subarachnoid space MCT8 was also associated with blood vessels and some fibrillar elements (Fig. 1g). MCT8 was also present at all ages in the membrane of choroid plexus epithelial cells, with strongest immunoreactivity in the apical portion and less in the cilia (Fig. 1h and Online Supplementary Resource 4). Weak MCT8 immunostaining was observed in the fenestrated vessels of the stroma (Online Supplementary Resource 4).

MCT8 was also expressed at all ages in the epithelium lining the lateral ventricles and the mesencephalic aqueduct (Online Supplementary Resource 4). The strongest intensity was present in the fourth ventricle, increasing considerably from GW20 onwards, mostly in the ventral region as shown in Fig. 1i for GW25. This figure shows the presence of MCT8 in the apical membrane and cytoplasm of ependymocytes facing the ventricles and with lesser intensity in cilia and basal processes running to the parenchyma. Increased immunostaining with advancing development was also observed in the neuropil of the periventricular region of all ventricles (Fig. 1i).

Our results confirm the presence of MCT8 in the human fetal BBB and BCSFB (Roberts et al. 2008; Wirth et al. 2009; Chan et al. 2011, 2014) and describe the presence of MCT8 to the outer CSFBB as indicated by its localization in leptomeningeal cells. Especially relevant to BBB transport was the presence of MCT8 associated with the microvessels and in the astrocytes surrounding them. Since these cells express DIO2 (Guadaño-Ferraz et al. 1997; Fliers et al. 2006), this observation suggests that T4 transport through the BBB is linked to T4 deiodination to T3 in the fetal human astrocytes.

MCT8 is expressed in the radial glia and Cajal Retzius cells in the developing cerebral cortex

Interestingly, MCT8 was strongly expressed in the RG spanning the cortical plate (Fig. 2a–d, f, g, and Online Supplementary Resource 4), with lower intensity in the subplate (Fig. 2a). MCT8 immunoreactivity was associated with RG immunopositive for nestin, vimentin, and GFAP (Fig. 2d–f, and Online Supplementary Resource 8). RG immunostaining intensity was variable among different cortical areas, and increased from GW14-16 to GW20 when MCT8 immunoreactivity was strong throughout all cerebral cortices (Fig. 2a–f and Online Supplementary Resource 4). Despite the high MCT8 immunoreactivity, from GW32 a decrease in the density and definition of MCT8 immunopositive RG basal processes was observed (Fig. 2g). MCT8 expression in the RG was also confirmed by the analysis of a single-cell transcriptomics database from isolated human RG cells. The data indicate that *MCT8/SLC16A2* is expressed in RG cells of the VZ and SVZ from GW16 to GW18 (Online Supplementary Resource 9). Interestingly, at all ages, weak MCT8

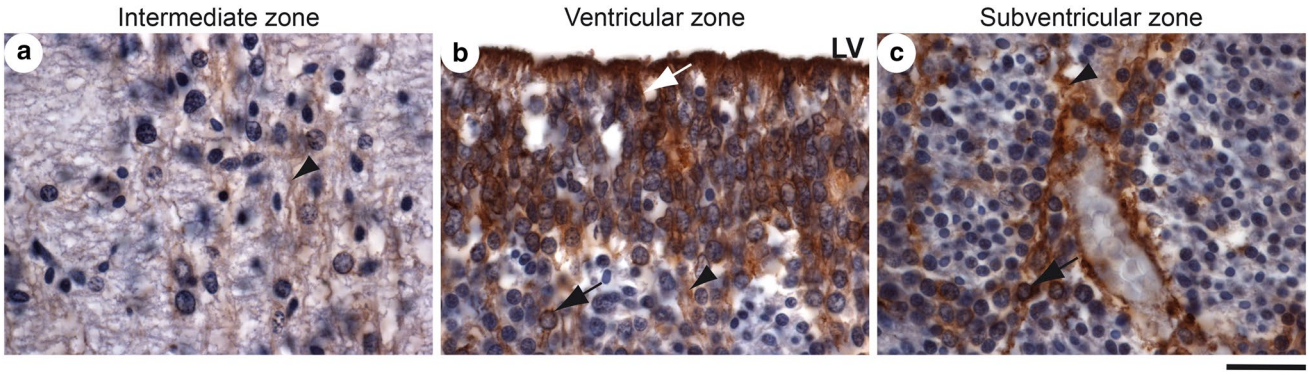

Fig. 4 MCT8 immunostaining in the intermediate, subventricular, and ventricular zones. Representative photomicrographs showing immunohistochemical staining (brown color) of MCT8 in the intermediate zone (**a**), in the VZ (**b**), and in the SVZ (**c**) in human fetus at GW20. Tissue sections were also counterstained with hematoxylin (blue color). Arrowheads in **a**–**c** point to RG basal processes. White arrow in **b** points to **a** RG soma immunopositive for MCT8 in the lateral ventricle surface, comprising the inner cerebrospinal fluid–brain barrier. Black arrows in **b** and **c** point to immunopositive precursor cells in the ventricular and subventricular zone, respectively. *LV* lateral ventricle. Scale bar represents 23 µm (**a**–**c**)

immunoreactivity was found in a reticulated framework in the marginal zone (MZ)/layer I, which corresponds to the basal end-feet of RG (Fig. 2h). Additionally, cells with the typical morphology and distribution of Cajal–Retzius cells staining for reelin (Marín-Padilla 2015) also expressed MCT8 (Fig. 2h, i, and Online Supplementary Resource 4).

Besides the RG, between GW16 and GW25 weak perinuclear MCT8 immunoreactivity was detected in some immature neurons in the cortical plate (Fig. 2c, and Online Supplementary Resource 4) and subplate (Online Supplementary Resource 4). From GW32, MCT8 neuronal immunoreactivity was more intense and mainly localized in the cell membrane (Fig. 2g and Online Supplementary Resource 4).

Given the involvement of RG in cell migration, we examined similar paths of cell migration. As in the cortical plate, strong MCT8 immunoreactivity was found in RG basal processes of the Cornu Ammonis (CA) region of the hippocampus (Fig. 3a and Online Supplementary Resource 4) and in the anterior extramural migratory stream (AEMS) fibers (Fig. 3e and Online Supplementary Resource 4). Also, moderate MCT8 immunoreactivity was found in the midline raphe glial fibers of the brainstem and to a lesser extent in a portion of the cellular component of this structure (Fig. 3i, m and Online Supplementary Resource 4). Furthermore, strong immunoreactivity was detected in nests of migrating granule cells of the presubiculum and subiculum (Fig. 3q, u and Online Supplementary Resource 4).

These data reinforce the possible participation of MCT8 in TH availability for RG basal processes and other cell structures, in order to facilitate TH action during the period of neuronal migration.

Localization of MCT8 in the intermediate zone, subventricular zone, and ventricular zone

Weak MCT8 immunostaining was present in the RG basal processes of the IZ at all ages (Fig. 4a and Online Supplementary Resource 4). From GW20, moderate MCT8 immunoreactivity was observed in GFAP + cells (Fig. 1c and Online Supplementary Resource 4). Strong staining, similar to the cortical plate, was present in the VZ and SVZ (Fig. 4b, c, and Online Supplementary Resource 4) in RG processes and cell bodies. Staining in the VZ was more prominent at the apical neuroepithelial surface (Fig. 4b).

Our results confirm the presence of MCT8 along the entire RG cell, from the VZ to the cortical surface through the IZ. MCT8 localization in RG and neuroepithelial cell bodies suggests a novel second entry pathway for TH to the brain parenchyma through the inner CSFBB.

MCT8 protein correlates with *MCT8* mRNA localization

The distribution of *MCT8* mRNA was analyzed by radioactive in situ hybridization at GW14, 16, 20, 32, and 38 in several brain regions. In all cases, there was a good correlation between the MCT8 immunoreactivity and mRNA. Higher content of hybridization grains corresponded to strongest MCT8 immunoreactivity, as shown at GW16 in the BBB (Fig. 5a), the choroid plexus (Fig. 5b) and SVZ and VZ (Fig. 5c). In situ hybridization for *MCT8* combined with immunohistochemistry for nestin clearly shows *MCT8* expression associated with nestin-immunopositive RG basal processes of the cortical plate (Fig. 5d).

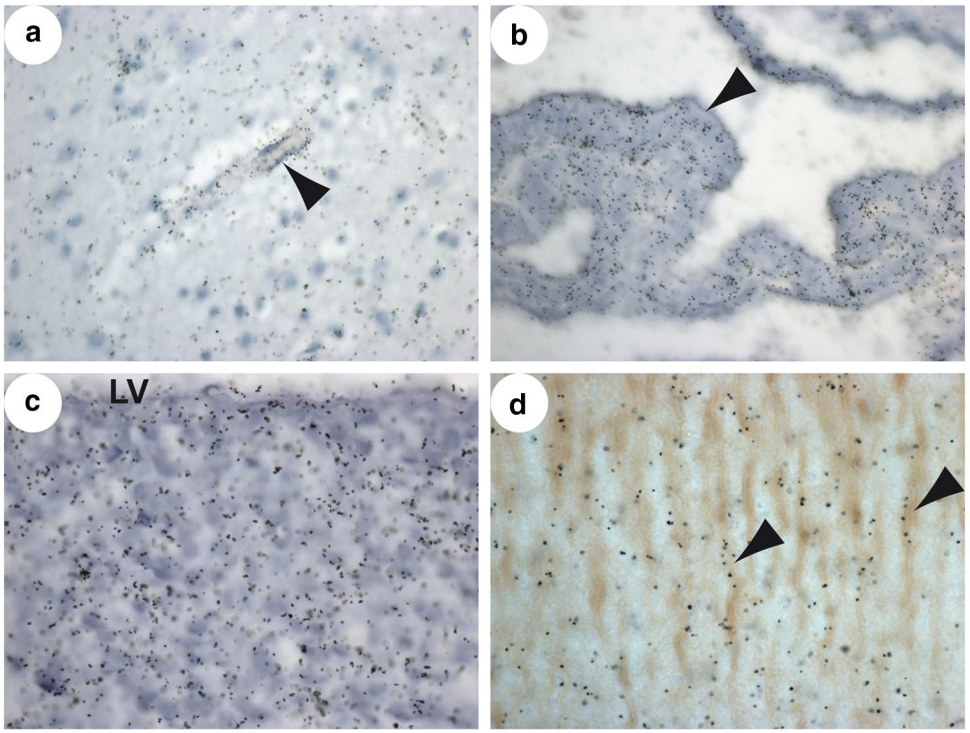

Fig. 5 *MCT8* mRNA expression in the human fetal brain. Representative photomicrographs showing *MCT8* mRNA expression (black grains) associated with blood vessels of the brainstem (**a**), the lateral ventricle choroid plexus (**b**), the VZ of the lateral ventricle (**c**) and the cerebral cortex (**d**) in fetuses at GW16. Note the high accumulation of hybridization grains on blood vessels (arrowhead in **a**), the choroid plexus (arrowhead in **b**) and in the VZ in **c**. In the cerebral cortex note the presence of hybridization grains along the RG basal processes immunopositive for nestin (arrowheads in **d**). *LV* lateral ventricle. Scale bar represents 50 µm (**a**, **b**) and 30 µm (**c**, **d**)

OATP1C1, DIO2, and DIO3 are expressed in the brain barriers and ventricular system

Similar to MCT8, OATP1C1, DIO2, and DIO3 were also detected associated with blood vessels in all regions at all prenatal ages (Fig. 6a–c and Online Supplementary Resources 5–7). Staining intensity was much lower than for MCT8 and some vessels were not stained (Online Supplementary Resources 5–7). From GW32 DIO2 immunoreactivity was found in astrocytes surrounding capillary vessels (Online Supplementary Resource 6). The strongest immunoreactivity for OATP1C1, DIO2, and DIO3 was present in the choroid plexus (Online Supplementary Resources 5–7), where epithelial cells showed an intense and homogeneous signal associated with the cell membrane, and moderate signal in the cytoplasm (Fig. 6d–f). In contrast to MCT8, OATP1C1, DIO2, and DIO3 had very weak or no immunoreactivity in stromal vessels of the choroid plexus (Fig. 6d–f and Online Supplementary Resources 5–7).

OATP1C1, DIO2, and DIO3 immunoreactivity was also observed with moderate intensity in leptomeningeal cells (Fig. 6g–i and Online Supplementary Resources 5–7) and blood vessels of the subarachnoid space (Fig. 6g–i).

In ependymocytes and tanycytes, the localization of OATP1C1 and DIO2 was similar to MCT8, gradually increasing up to GW20 (Fig. 6j, k, and Online Supplementary Resources 5 and 6). However, in ependymocytes and tanycytes DIO3 showed strong immunostaining at all ages in the soma and cilia, and also in the processes running into the periventricular stroma of all the cerebral ventricles (Fig. 6l and Online Supplementary Resource 7).

These results suggest that similar to MCT8, OATP1C1 and deiodinases are located in several cells composing all the brain barriers. In contrast to MCT8, the expression of OATP1C1 and deiodinases is weak in the BBB and much stronger in other fetal barriers.

Radial glial cells in the developing cerebral cortex express OATP1C1, DIO2, and DIO3

OATP1C1, DIO2, and DIO3 were observed, as MCT8, in nestin-immunopositive RG basal processes of the cortical plate (Fig. 6m–o, and Online Supplementary Resources 5–7) and the subplate at all ages (Data not shown). DIO3 displayed the strongest staining. In the MZ/layer I, OATP1C1, DIO2, and DIO3 were also detected in the RG end-feet, and Cajal–Retzius cells (Fig. 6p–r, and Online Supplementary Resources 5–7). OATP1C1, DIO2, and DIO3 were also detected, as MCT8, in the RG basal processes of the hippocampal CA region (Fig. 3b–d and Online Supplementary Resources 5–7) and in the AEMS fibers (Fig. 3f–h and Online Supplementary Resources 5–7), OATP1C1 with the lowest immunostaining in this last structure (Fig. 3f and Online Supplementary Resources 5–7). Expression of OATP1C1 and DIO2 in the RG was also confirmed by analysis of the single cell genomics data from (Pollen et al. 2015)

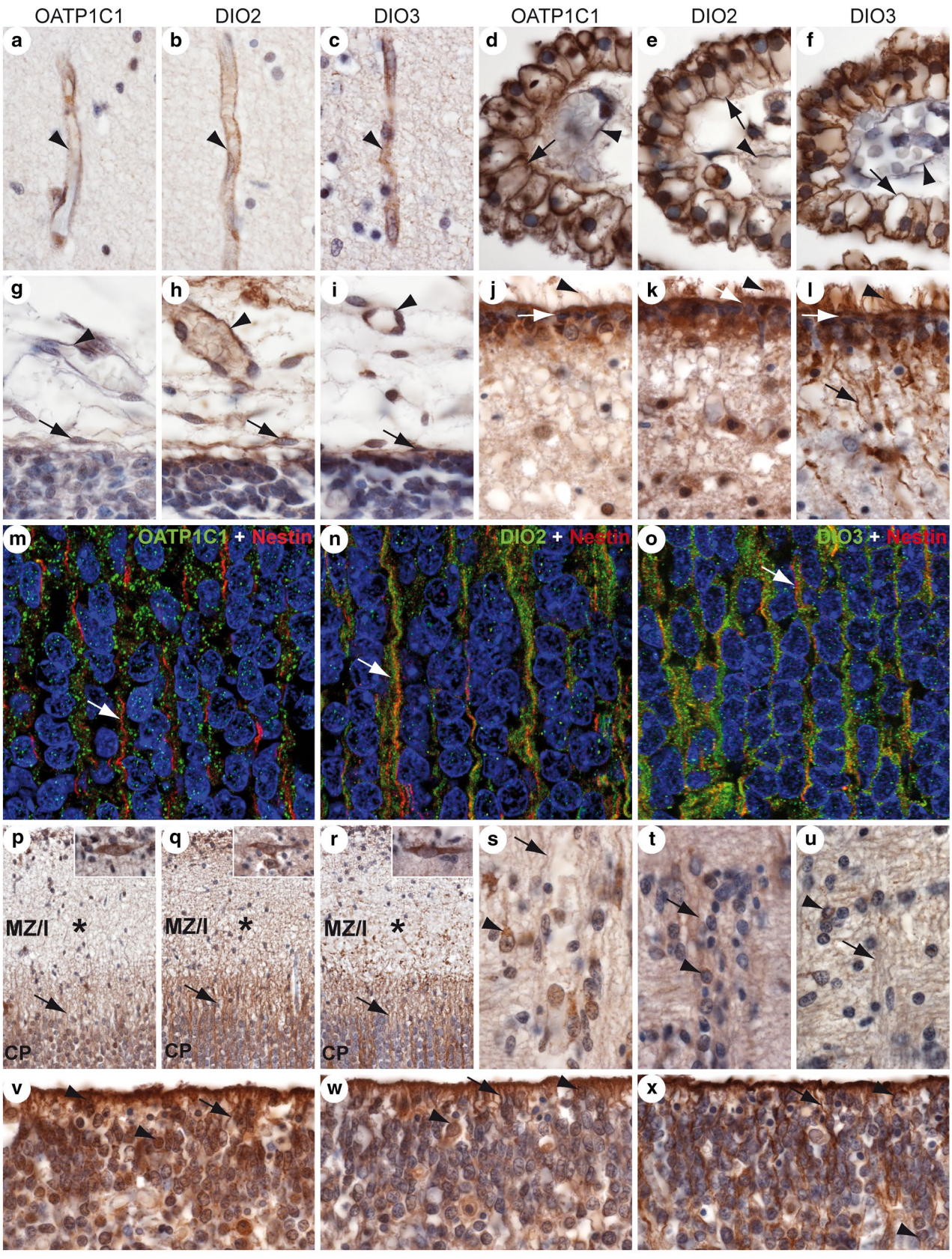
OATP1C1
DIO2
DIO3
OATP1C1
DIO2
DIO3
a
b
c
d
e
f
g
h
i
j
k
l
m
OATP1C1 + Nestin
n
DIO2 + Nestin
o
DIO3 + Nestin
p
q
r
s
t
u
MZ/I
*
CP
v
w
x

◂**Fig. 6** OATP1C1, DIO2, and DIO3 immunostaining in fetal cerebral barriers, radial glia, and neural cells. Representative photomicrographs showing immunohistochemical (brown color) and immunofluorescence (green color) staining of OATP1C1 (**a**, **d**, **g**, **j**, **m**, **p**, **s**, **v**), DIO2 (**b**, **e**, **h**, **k**, **n**, **q**, **t**, **w**) and DIO3 (**c**, **f**, **i**, **l**, **o**, **r**, **u**, **x**) in the BBB (**a**–**c**), the blood-cerebrospinal fluid (**d**–**f**), meninges and outer cerebrospinal fluid–brain barrier (**g**–**i**), lateral ventricle ependymocytes (**j**–**l**), RG basal processes in the cerebral cortex (**m**–**r**), Cajal–Retzius cells (**p**–**r**), radial RG processes and neural cells in the intermediate zone (**s**–**u**) and neural precursors and RG in the VZ (**v**–**x**) in control fetuses at GW14 (**g**–**i**, **m**–**o**), GW16 (**d**–**f**) and GW20 (**a**–**c**, **j**–**l**, **p**–**x**). Arrowheads in **a**–**c** indicate the weak expression of OATP1C1 and deiodinases associated with blood vessels. In **d**–**f**, note the strong expression of OATP1C1 and deiodinases in the epithelial choroid plexus cells (arrows) and the weak expression in fenestrated capillaries in the choroid plexus stroma (arrowheads). In **g**–**i**, OATP1C1 and deiodinases immunostaining in leptomeningeal cells (arrows) and capillary vessels of the subarachnoid space (arrowheads). In **g** note the lower immunoreactivity for OATP1C1 in leptomeningeal cells in comparison to deiodinases and MCT8. In **j**–**l** OATP1C1 and deiodinases immunoreactivity in ependymocytes lining the lateral ventricle (white arrows) and in the cilia (arrowheads). Note the strong DIO3 expression in the long basal processes (black arrow in **l**). Arrows in **m**–**x** point to OATP1C1 and deiodinases immunoreactivity in RG basal processes immunopositive for nestin (**m**–**o**, nestin in red). Arrowheads in **s**–**x** point to deiodinases and OATP1C1 immunoreactivity in neural cells. Note the low OATP1C1 expression in the RG basal processes in **p**, **s** and **v** and the low expression of all proteins in the RG basal processes in the intermediate zone (**s**–**u**). In **p**–**r** deiodinases and OATP1C1 immunoreactivity in the basal endfeet of RG (arrows) and in the endings forming a reticulated framework in the MZ/I (asterisks). Insets in **p**–**r** show deiodinases and OATP1C1 immunostaining in Cajal–Retzius cells. *CP* cortical plate, *MZ/I* marginal zone/layer I. Scale bar represents 22 µm (**a**–**l**, **s**–**x**), 12 µm (**m**–**o**), and 56 µm (**p**–**r**)

(Online Supplementary Resource 9). Nineteen percent of RG in the VZ and 16% in the SVZ expressed *OATP1C1/SLCO1C1*, and 95% of these cells expressed the glia marker gene *VIM*. Interestingly, there was a high correlation between *OATP1C1/SLCO1C1* expression and DIO2 (30% in the VZ and 19% in the SVZ coexpressed both genes). The glial nature of most DIO2-expressing cells was also confirmed by *VIM* coexpression.

OATP1C1, DIO2, and DIO3 were also observed in the midline raphe glial fibers (Fig. 3j–l, n–p and Online Supplementary Resources 5–7) of the brainstem, and unlike MCT8 and DIO3, moderate OATP1C1, and moderate to strong DIO2 immunoreactivity were observed in migrating neurons of the raphe nuclear complex (Fig. 3j, k, n, o and Online Supplementary Resources 5–7). OATP1C1, DIO2, and DIO3 immunoreactivity was minimal in migrating granule cell nests in the subiculum and presubiculum (Fig. 3r–t, v–x and Online Supplementary Resources 5–7).

OATP1C1 presented moderate, and DIO2 and DIO3 strong immunoreactivity in some immature neurons in the cortical plate and subplate (Online Supplementary Resources 10 and 5–7).

All these data suggest that RG, Cajal–Retzius cells, and cortical neurons could get T4 through MCT8 and OATP1C1 and autonomously generate T3 and degrade TH through deiodinases, thereby regulating their T3 and T4 content.

OATP1C1, DIO2, and DIO3 are also present in the intermediate zone, subventricular zone and ventricular zone

At all ages, OATP1C1 and DIO2 displayed weak immunoreactivity in the RG processes of the IZ, SVZ, and VZ (Fig. 6s, t, v, w, and Online Supplementary Resources 5 and 6). DIO3 showed weak immunoreactivity in the RG processes of the IZ (Fig. 6u, and Online Supplementary Resource 7), and moderate signal in the SVZ and VZ (Fig. 6x and Online Supplementary Resource 7). OATP1C1, DIO2, and DIO3 also presented moderate to strong immunoreactivity in the soma of RG in the VZ (Fig. 6v–x, and Online Supplementary Resources 5–7). In the IZ OATP1C1, DIO2, and DIO3 immunoreactivity was observed in cells near RG processes, probably migrating cells (Fig. 6s–u, Online Supplementary Resources 5–7). GFAP immunopositive cells of the IZ also showed OATP1C1 and DIO2 from GW32, as MCT8, but not DIO3 (Online Supplementary Resources 5 and 6). In addition, at all studied ages moderate OATP1C1, DIO2, and DIO3 signals were observed in the cytoplasm of many cells and in the neuropil in both the VZ (Fig. 6v–x and Online Supplementary Resources 5–7) and SVZ (Online Supplementary Resources 5–7).

These data suggest that, as MCT8, OATP1C1 would allow the passage of T4 from the CSF to the RG, i.e., crossing the inner CSFBB. From the RG, TH could pass to the cells in the VZ and SVZ and to the migrating cells and astrocytes in the IZ. On the other hand, RG, VZ, and SVZ neural cells, as well as astrocytes and migrating cells in the IZ would be able to activate or inactivate TH intracellularly by deiodinases.

Discussion

A fundamental question in TH action in the brain is how TH cross the brain barriers and which cells transform T4 into the active hormone T3 in the brain. In rodents, TH cross the BBB through the OATP1C1 and MCT8 transporters, while astrocytic DIO2 generates T3 from T4. Lack of knowledge of these pathways during early human development precludes a clear understanding of the relative roles of maternal and fetal hormones in brain development, and the pathogenesis of the Allan–Herndon–Dudley syndrome caused by *MCT8/SLC16A2* mutations. Here, by analyzing the expression of TH transporters and deiodinases we propose a novel model (Fig. 7) of TH transport and metabolism

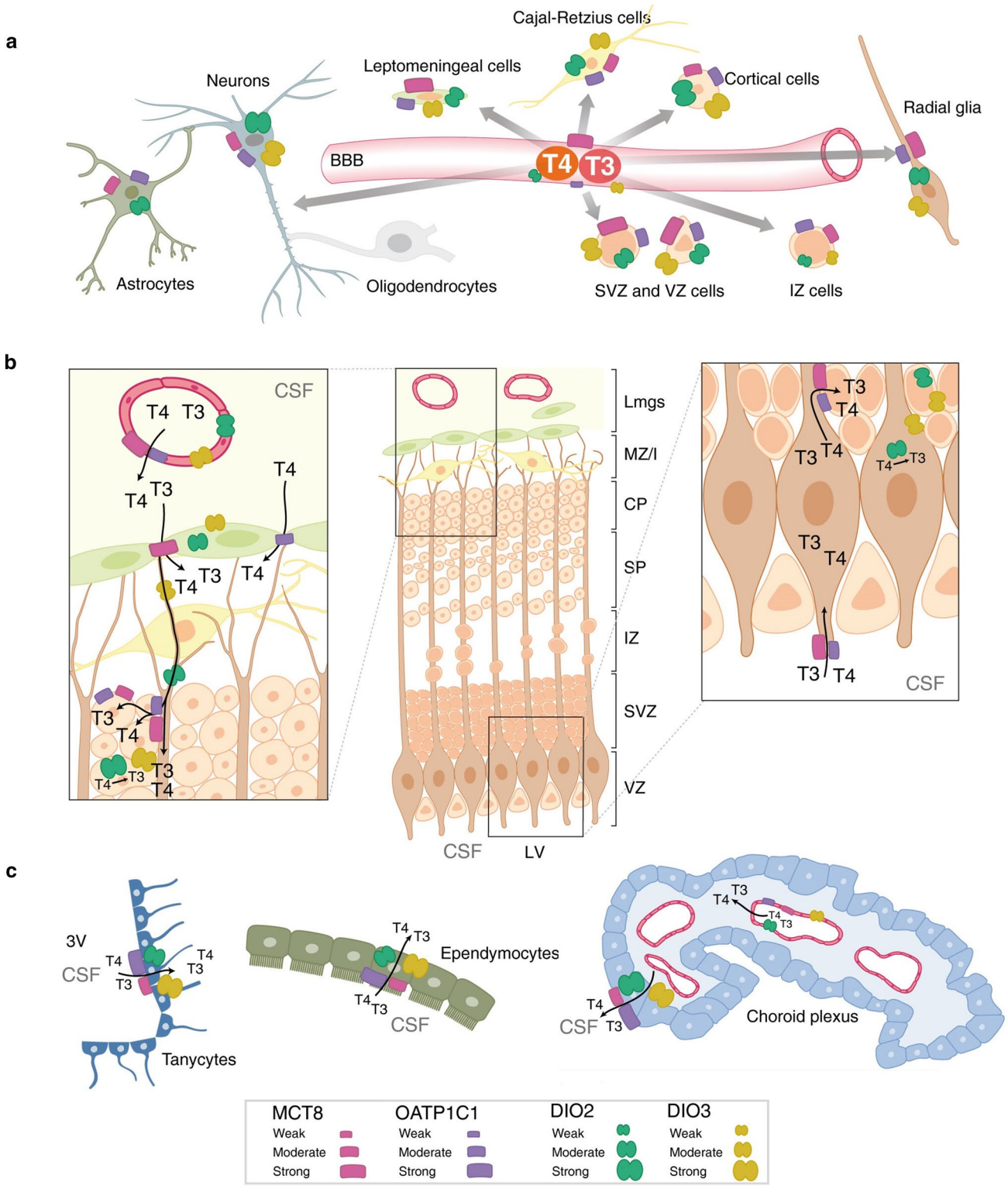

in the developing human brain with a central role played by the RG in local T3 formation.

Our model proposes that during prenatal stages, circulating TH enter the brain not only through the two previously reported brain barriers, the BBB and the BCSFB, but also through two other brain barriers, the outer CSFBBs and the inner CSFBBs, which disappear later in development.

The fetal CSF contains a high concentration of plasma proteins (Adinolfi and Haddad 1977) during the processes of neurogenesis and the formation of the cortical plate

◂**Fig. 7** Putative model describing thyroid hormones delivery routes for neural cells in the human fetal brain. Scheme illustrating the localization of MCT8, OATP1C1, DIO2 and DIO3 at fetal stages. The immunolabeling intensity of each protein is shown by symbols of different sizes indicating its abundance in every cell type. Immunoreactivity intensity was qualitatively evaluated as compared to its maximum signal observed in all regions and ages studied. **a** T4 and T3 are transported through the BBB by MCT8 and, to a lesser extent, by OATP1C1, to reach different neural cells that express MCT8, OATP1C1 and DIO2 and DIO3. **b** Middle panel schematizes histology from the VZ to the cortical surface. Left panel depicts a possible T4 and T3 entry pathway by MCT8 and OATP1C1 from capillaries to the CSF, and then to the brain parenchyma through the leptomeningeal cells at the outer cerebrospinal fluid–brain barrier. Once in the parenchyma, T4 and T3 could pass to the extracellular fluid or be captured by the RG endfeet and delivered to cortical neurons by OATP1C1 and MCT8, both located in RG basal processes and neurons. In the leptomeningeal and cortical cells, T4 and T3 concentrations could be regulated by DIO2 and DIO3. Right panel shows the possible T4 and T3 flow from CSF to the cells in the VZ by OATP1C1 and MCT8 in neuroepithelial and/or RG cells forming the inner cerebrospinal fluid–brain barrier. In neuroepithelial cells, RG and VZ cells, T4 and T3 concentrations could be regulated by DIO2 and DIO3. **c** Right panel shows the localization of transporters and deiodinases in the choroid plexus, and the possible flow of T4 and T3 from the fenestrated capillaries in the choroid plexus to the CSF through the epithelial cells that conform the blood–cerebrospinal fluid barrier. Left and middle panels show that T4 and T3 could also reach the brain parenchyma by MCT8 and OATP1C1 through the ependymocytes and tanycytes, where T4 and T3 concentrations could be regulated by DIO2 and DIO3. *BBB* Blood–brain barrier, *CSF* Cerebrospinal fluid, *Lmgs* Leptomeninges, *MZ/I* Marginal zone/layer I, *CP* Cortical plate, *SP* Subplate, *IZ* Intermediate zone, *SVZ* Subventricular zone, *VZ* Ventricular zone, *LV* Lateral ventricle, 3 *V* Third ventricle

(Saunders et al. 1999), and the outer and inner CSFBBs barriers control the diffusion of CSF molecules to the brain parenchyma. Important signaling molecules and growth factors enter the brain through these barriers. As an example, retinoic acid produced in the meninges by the enzyme ALDH1A2 is captured by the RG end-feet in contact with the pia mater, and is delivered along the basal processes to the RG soma located in the SVZ and VZ (Siegenthaler et al. 2009). On the other hand, the retinoic acid precursor all-*trans* retinol diffuses from the CSF to the neuroepithelial cells of the VZ expressing the T3-regulated enzyme ALDH1A3 (Gil-Ibáñez et al. 2014) that generates retinoic acid in the control of neurogenesis (Alonso et al. 2011; Smith et al. 2001). Similarly, we here propose that MCT8 and OATP1C1, located in the outer and inner CSFBBs, contribute to the passage of TH from the CSF to the brain parenchyma. Our model implies that the modulation of TH availability in the human prenatal brain differs from that proposed for the rodent postnatal brain. In the latter, astrocytes expressing *Dio2* control the generation of T3, and neurons expressing *Dio3* control the degradation of T4 and T3. Our present results suggest that different cell types in humans have the ability to control the intracellular generation of T3 from T4 and their degradation. Studies in rats have shown that maternal thyroxine is important for cortical neurogenesis even before onset of fetal thyroid gland function, and that *Mct8*, *Thra*, and *Dio2* are expressed in the VZ (Mohan et al. 2012).

Among the most novel and relevant results of this study is the strong expression of MCT8 and to a lesser extent of OATP1C1, DIO2, and DIO3 in the basal processes of RG in the cerebral cortex, in Cajal–Retzius cells and in the IZ, SVZ, and VZ. The RG, which need TH for proper maturation (Nicholson and Altman 1972; Martinez-Galan et al. 1997) would also be crucial for the delivery of TH to immature neurons throughout the cerebral cortex and to cells undergoing proliferation or differentiation in the SVZ and VZ. The Cajal–Retzius cells, essential for the regulation of cortical migration, are cellular targets of T3, expressing genes under TH control, such as *Reln*, *Dab1* (Alvarez-Dolado et al. 1999; Pathak et al. 2011), and many other genes (Gil-Ibáñez et al. 2017). These data agree with the role of TH demonstrated in rodents on development of cortical cytoarchitecture (Lavado-Autric et al. 2003; Ausó et al. 2004; Guadaño-Ferraz et al. 1994) as well as in the proliferation of neural precursors in the VZ (Stenzel et al. 2014). Also in chicken embryos MCT8 knockdown in the optic tectum is associated with the disorganization of the RG basal processes, reduced reelin signaling, and disruption of neural progenitor migration (Vancamp et al. 2017).

The presence of MCT8, OATP1C1, DIO2, and DIO3 in other migratory streams in the hippocampus and brainstem, and migrating cells in the subiculum and presubiculum, suggests that these proteins control the local concentrations of TH to regulate cell migration also in these regions. It is remarkable that in the cerebral cortex and most brain regions analyzed, increasing immunoreactivity for these proteins is observed between GW14 and 16, with maximal intensity at around GW20, similar to the increase in T3 receptor in the whole brain, and T3 concentrations and DIO2 activity in the cerebral cortex (Bernal and Pekonen 1984; Kester et al. 2004). These events occur during the period of neuronal migration and the beginning of gliogenesis (Sidman and Rakic 1973). Although the goal of our present study was to analyze the transport routes and their coupling with deiodinases, knowledge of the distribution of TH receptors would have provided a wealth of information on the target cells and the role of TH. These studies are however, difficult to perform at the protein level due to the lack of specificity of TH receptor antibodies. With the possibility of searching a single-cell genomics database we looked at the expression of the two TH receptor genes *THRA* and *THRB*. The data (Online Supplementary Resource 9) show that *THRA* and *THRB* were also expressed in the VZ (14% of the cells for *THRA* and 10% for *THRB*) and SVZ (20% for *THRA* and 7% for *THRB*) at GW16-18. Their patterns of expression showed

no overlap, and each receptor was expressed in different sets of cells. However, their expression was not clearly correlated with specific transporters or cell markers, showing scattered distribution. It is possible that the receptors in these cells and at these stages of development still remain in the unliganded, repressor state. The increased receptor and T3 concentration occurring from GW12 to GW20 (Bernal and Pekonen 1984; Kester et al. 2004) may be more related to events of terminal differentiation in other areas. This is not surprising in view that at the same fetal ages the cerebral cortex accumulates T3, whereas the cerebellar cortex keeps T3 very low (Kester et al. 2004), presumably resulting in a liganded receptor in the former and unliganded in the latter.

The increased OATP1C1, DIO2, and DIO3 content at midgestation in the cerebral cortex agrees with other studies (Karmarkar et al. 1993; Chan et al. 2002, 2011; Kester et al. 2004). Differences between our findings and those of (Chan et al. 2011) showing constant amounts of *MCT8* mRNA between GW7 and 20, may be due to post-transcriptional regulation.

Knowledge on the expression of MCT8, OATP1C1, DIO2, and DIO3 in the human brain is important to understand the pathophysiological mechanisms caused by *MCT8/SLC16A2* disruption underlying the Allan–Herndon–Dudley Syndrome (Allan et al. 1944; Schwartz et al. 2005). The *Mct8* knockout mice are not neurologically impaired as do patients with this syndrome. Functional studies in rodents indicate that transport across the BBB is the main TH access route to the brain (Chanoine et al. 1992). It is thought that in the mouse, abundant expression of OATP1C1 in the BBB, unlike the situation in primates, compensates for the lack of MCT8 (Mayerl et al. 2014). In our study the weak expression of OATP1C1 in the prenatal human BBB, in contrast with what is observed in rodents, and its abundant expression in epithelial cells of the choroid plexus, ependymal cells, tanycytes and leptomeningeal cells, confirms that OATP1C1 has a secondary role in the entry of circulating TH to the human fetal brain (Roberts et al. 2008). This would explain why MCT8 deficiency in humans results in brain morphological alterations at prenatal stages (López-Espíndola et al. 2014) with delayed maturation of the cerebral cortex and cerebellum, hypomyelination, and altered synaptogenesis. These defects underlie the serious neurological disorders (Matheus et al. 2015) caused by restriction of TH to the brain since early developmental stages, thus impairing neural cell differentiation and migration.

The present study provides insight into the role of MCT8, OATP1C1, DIO2, and DIO3 in the control of the passage of appropriate concentrations of TH through the brain barriers during most part of the prenatal period. In the human fetal brain, we observed an intense expression of MCT8 and a minimal expression of OATP1C1, DIO2, and DIO3 in the BBB, which suggests the importance of MCT8 in the transport of TH to the brain during development. Interestingly, this is not observed in other species as the chicken, in which neither *Mct8* nor *Oatp1c1* is expressed in the BBB during development (Geysens et al. 2012) but *Lat1/Slc7a5* amino acid transporter is (Van Herck et al. 2015). In chicken, as in humans, *Mct8, Oatp1c1, Dio2, Dio3,* and *Lat1* are expressed in the choroid plexus (Van Herck et al. 2015; Delbaere et al. 2016; Geysens et al. 2012; Bourgeois et al. 2016). While it is possible that other transporters besides MCT8 and OATP1C1 may be of functional importance in the human, the analysis of single RG cells (Online Supplemental Resource 9) indicates that only small percentage of cells express alternative transporters. In addition, DIO2 coexpression with OATP1C1 reinforces the importance of this transporter in TH metabolism and the provision of local T3.

The outer and inner CSFBBs appear alternative entry pathways that may supply TH during human neurodevelopment, and future studies are needed to determine the contribution of these new entry pathways in the delivery of TH into the prenatal brain. The knowledge of alternative entry routes where MCT8 is highly expressed allows to identify new cellular targets for gene therapies for diseases involving brain hypothyroidism.

Acknowledgements We are very grateful to the subjects' parents who gave their consent to using the brain tissues for this investigation. We are also indebted to the IdiPAZ Biobank integrated into the Spanish Biobank Network (http://www.redbiobancos.es) and the Wolfson Medical Center, Holon, Israel, and the Sackler School of Medicine, Tel Aviv, Israel for the generous gifts of clinical samples used in this work. The IdiPAZ Biobank is supported by Instituto de Salud Carlos III, Spanish Health Ministry (Retic RD09/0076/00073) and Farmaindustria, through the Cooperation Program in Clinical and Translational Research of the Community of Madrid. We thank Drs. Soledad Bárez-López, José Miguel Cosgaya, Estrella Rausell and Ana Montero-Pedrazuela for the careful reading of the manuscript and their helpful suggestions, and Javier Pérez for his help on the artwork. This work was supported by Grants from the Spanish Plan Nacional de I+D+i (Grant numbers SAF2014-54919-R and SAF2017-86342-R to A.GF and J.B), and the Center for Biomedical Research on Rare Diseases (Ciberer), Instituto de Salud Carlos III, Madrid, Spain and the Sherman Foundation (OTR02211 to A.GF). D.LE is a recipient of a fellowship from "Fellowship Training Program for Advanced Human Capital, BECAS CHILE" from the National Commission for Scientific and Technological Research (CONICYT), Gobierno de Chile. The cost of this publication has been paid in part by FEDER funds.

Compliance with ethical standards

Conflict of interest The authors declare that they have no conflict of interest.

Ethical approval All procedures performed involving human samples were in accordance with the ethical standards of our institution research ethic committee (Consejo Superior de Investigaciones Científicas, permit SAF2011-25608) and the 1964 Helsinki Declaration and its later amendments or comparable ethical standards.

References

Adinolfi M, Haddad SA (1977) Levels of plasma proteins in human and rat fetal CSF and the development of the blood–CSF barrier. Neuropadiatrie 8(4):345–353. https://doi.org/10.1055/s-0028-1091530

Alkemade A, Friesema EC, Unmehopa UA, Fabriek BO, Kuiper GG, Leonard JL, Wiersinga WM, Swaab DF, Visser TJ, Fliers E (2005) Neuroanatomical pathways for thyroid hormone feedback in the human hypothalamus. J Clin Endocrinol Metab 90(7):4322–4334. https://doi.org/10.1210/jc.2004-2567

Alkemade A, Friesema EC, Kalsbeek A, Swaab DF, Visser TJ, Fliers E (2011) Expression of thyroid hormone transporters in the human hypothalamus. J Clin Endocrinol Metab 96(6):E967–E971. https://doi.org/10.1210/jc.2010-2750

Allan W, Herndon CN, Dudley FC (1944) Some examples of the inheritance of mental deficiency: apparently sex-linked idiocy and microcephaly. Am J Ment Defic 48:325–334

Alonso MI, Martin C, Carnicero E, Bueno D, Gato A (2011) Cerebrospinal fluid control of neurogenesis induced by retinoic acid during early brain development. Dev Dyn 240(7):1650–1659. https://doi.org/10.1002/dvdy.22657

Alvarez-Dolado M, Ruiz M, Del Río JA, Alcántara S, Burgaya F, Sheldon M, Nakajima K, Bernal J, Howell BW, Curran T, Soriano E, Muñoz A (1999) Thyroid hormone regulates reelin and dab1 expression during brain development. J Neurosci 19(16):6979–6993

Ausó E, Lavado-Autric R, Cuevas E, Del Rey FE, Morreale de Escobar G, Berbel P (2004) A moderate and transient deficiency of maternal thyroid function at the beginning of fetal neocorticogenesis alters neuronal migration. Endocrinology 145(9):4037–4047. https://doi.org/10.1210/en.2004-0274

Bayer S, Altman J (2003) The human brain during the third trimester, 1st edn. CRC Press, USA

Bayer S, Altman J (2005) The human brain during the second trimester, 1st edn. CRC Press, USA

Bernal J (2007) Thyroid hormone receptors in brain development and function. Nat Clin Pract Endocrinol Metab 3(3):249–259. https://doi.org/10.1038/ncpendmet0424

Bernal J, Guadaño-Ferraz A (2002) Analysis of thyroid hormone-dependent genes in the brain by in situ hybridization. Methods Mol Biol 202:71–90. https://doi.org/10.1385/1-59259-174-4:71

Bernal J, Pekonen F (1984) Ontogenesis of the nuclear 3,5,3′-triiodothyronine receptor in the human fetal brain. Endocrinology 114(2):677–679. https://doi.org/10.1210/endo-114-2-677

Bernal J, Guadaño-Ferraz A, Morte B (2015) Thyroid hormone transporters—functions and clinical implications. Nat Rev Endocrinol 11(7):406–417. https://doi.org/10.1038/nrendo.2015.66

Bourgeois NM, Van Herck SL, Vancamp P, Delbaere J, Zevenbergen C, Kersseboom S, Darras VM, Visser TJ (2016) Characterization of chicken thyroid hormone transporters. Endocrinology 157(6):2560–2574. https://doi.org/10.1210/en.2015-2025

Brochner CB, Holst CB, Mollgard K (2015) Outer brain barriers in rat and human development. Front Neurosci 9:75. https://doi.org/10.3389/fnins.2015.00075

Calvo R, Obregon MJ, Ruiz de Oña C, Escobar del Rey F, Morreale de Escobar G (1990) Congenital hypothyroidism, as studied in rats. Crucial role of maternal thyroxine but not of 3,5,3′-triiodo-L-thyronine in the protection of the fetal brain. J Clin Invest 86(3):889–899. https://doi.org/10.1172/jci114790

Ceballos A, Belinchón MM, Sánchez-Mendoza E, Grijota-Martínez C, Dumitrescu AM, Refetoff S, Morte B, Bernal J (2009) Importance of monocarboxylate transporter 8 for the blood–brain barrier-dependent availability of 3,5,3′-triiodo-L-thyronine. Endocrinology 150(5):2491–2496. https://doi.org/10.1210/en.2008-1616

Chan S, Kachilele S, McCabe CJ, Tannahill LA, Boelaert K, Gittoes NJ, Visser TJ, Franklyn JA, Kilby MD (2002) Early expression of thyroid hormone deiodinases and receptors in human fetal cerebral cortex. Brain Res Dev Brain Res 138(2):109–116

Chan SY, Martin-Santos A, Loubiere LS, Gonzalez AM, Stieger B, Logan A, McCabe CJ, Franklyn JA, Kilby MD (2011) The expression of thyroid hormone transporters in the human fetal cerebral cortex during early development and in *N*-Tera-2 neurodifferentiation. J Physiol 589(Pt 11):2827–2845. https://doi.org/10.1113/jphysiol.2011.207290

Chan SY, Hancox LA, Martin-Santos A, Loubiere LS, Walter MN, Gonzalez AM, Cox PM, Logan A, McCabe CJ, Franklyn JA, Kilby MD (2014) MCT8 expression in human fetal cerebral cortex is reduced in severe intrauterine growth restriction. J Endocrinol 220(2):85–95. https://doi.org/10.1530/JOE-13-0400

Chanoine JP, Alex S, Fang SL, Stone S, Leonard JL, Korhle J, Braverman LE (1992) Role of transthyretin in the transport of thyroxine from the blood to the choroid plexus, the cerebrospinal fluid, and the brain. Endocrinology 130(2):933–938. https://doi.org/10.1210/endo.130.2.1733735

Crantz FR, Silva JE, Larsen PR (1982) An analysis of the sources and quantity of 3,5,3′-triiodo-L-thyronine specifically bound to nuclear receptors in rat cerebral cortex and cerebellum. Endocrinology 110(2):367–375. https://doi.org/10.1210/endo-110-2-367

Delbaere J, Van Herck SL, Bourgeois NM, Vancamp P, Yang S, Wingate RJ, Darras VM (2016) Mosaic expression of thyroid hormone regulatory genes defines cell type-specific dependency in the developing chicken cerebellum. Cerebellum 15(6):710–725. https://doi.org/10.1007/s12311-015-0744-y

DeLong GR (1993) Effects of nutrition on brain development in humans. Am J Clin Nutr 57(2 Suppl):286S–290S

Dratman MB, Crutchfield FL, Schoenhoff MB (1991) Transport of iodothyronines from bloodstream to brain: contributions by blood:brain and choroid plexus:cerebrospinal fluid barriers. Brain Res 554(1–2):229–236

Dumitrescu AM, Refetoff S (2013) The syndromes of reduced sensitivity to thyroid hormone. Biochem Biophys Acta 1830(7):3987–4003. https://doi.org/10.1016/j.bbagen.2012.08.005

Dumitrescu AM, Liao XH, Best TB, Brockmann K, Refetoff S (2004) A novel syndrome combining thyroid and neurological abnormalities is associated with mutations in a monocarboxylate transporter gene. Am J Hum Genet 74(1):168–175. https://doi.org/10.1086/380999

Dumitrescu AM, Liao XH, Weiss RE, Millen K, Refetoff S (2006) Tissue-specific thyroid hormone deprivation and excess in monocarboxylate transporter (mct) 8-deficient mice. Endocrinology 147(9):4036–4043. https://doi.org/10.1210/en.2006-0390

Fliers E, Alkemade A, Wiersinga WM, Swaab DF (2006) Hypothalamic thyroid hormone feedback in health and disease. Prog Brain Res 153:189–207. https://doi.org/10.1016/S0079-6123(06)53011-0

Friesema EC, Ganguly S, Abdalla A, Manning Fox JE, Halestrap AP, Visser TJ (2003) Identification of monocarboxylate transporter 8 as a specific thyroid hormone transporter. J Biol Chem 278(41):40128–40135. https://doi.org/10.1074/jbc.M300909200

Friesema EC, Grueters A, Biebermann H, Krude H, von Moers A, Reeser M, Barrett TG, Mancilla EE, Svensson J, Kester MH, Kuiper GG, Balkassmi S, Uitterlinden AG, Koehrle J, Rodien P, Halestrap AP, Visser TJ (2004) Association between mutations in a thyroid hormone transporter and severe X-linked psychomotor retardation. Lancet 364(9443):1435–1437. https://doi.org/10.1016/S0140-6736(04)17226-7

Friesema EC, Visser TJ, Borgers AJ, Kalsbeek A, Swaab DF, Fliers E, Alkemade A (2012) Thyroid hormone transporters and deiodinases in the developing human hypothalamus. Eur J Endocrinol 167(3):379–386. https://doi.org/10.1530/EJE-12-0177

Galton VA, Wood ET, St Germain EA, Withrow CA, Aldrich G, St Germain GM, Clark AS, St Germain DL (2007) Thyroid hormone homeostasis and action in the type 2 deiodinase-deficient rodent brain during development. Endocrinology 148(7):3080–3088. https://doi.org/10.1210/en.2006-1727

Gereben B, Zeold A, Dentice M, Salvatore D, Bianco AC (2008) Activation and inactivation of thyroid hormone by deiodinases: local action with general consequences. Cell Mol Life Sci 65(4):570–590. https://doi.org/10.1007/s00018-007-7396-0

Geysens S, Ferran JL, Van Herck SL, Tylzanowski P, Puelles L, Darras VM (2012) Dynamic mRNA distribution pattern of thyroid hormone transporters and deiodinases during early embryonic chicken brain development. Neuroscience 221:69–85. https://doi.org/10.1016/j.neuroscience.2012.06.057

Gil-Ibáñez P, Bernal J, Morte B (2014) Thyroid hormone regulation of gene expression in primary cerebrocortical cells: role of thyroid hormone receptor subtypes and interactions with retinoic acid and glucocorticoids. PLoS One 9(3):e91692. https://doi.org/10.1371/journal.pone.0091692

Gil-Ibáñez P, García-García F, Dopazo J, Bernal J, Morte B (2017) Global transcriptome analysis of primary cerebrocortical cells: identification of genes regulated by triiodothyronine in specific cell types. Cereb Cortex 27(1):706–717. https://doi.org/10.1093/cercor/bhv273

Grijota-Martínez C, Díez D, Morreale de Escobar G, Bernal J, Morte B (2011) Lack of action of exogenously administered T3 on the fetal rat brain despite expression of the monocarboxylate transporter 8. Endocrinology 152(4):1713–1721. https://doi.org/10.1210/en.2010-1014

Guadaño-Ferraz A, Escobar del Rey F, Morreale de Escobar G, Innocenti GM, Berbel P (1994) The development of the anterior commissure in normal and hypothyroid rats. Brain Res Dev Brain Res 81(2):293–308

Guadaño-Ferraz A, Obregon MJ, St Germain DL, Bernal J (1997) The type 2 iodothyronine deiodinase is expressed primarily in glial cells in the neonatal rat brain. Proc Natl Acad Sci USA 94(19):10391–10396

Howard D, La Rosa FG, Huang S, Salvatore D, Mulcahey M, Sang-Lee J, Wachs M, Klopper JP (2011) Consumptive hypothyroidism resulting from hepatic vascular tumors in an athyreotic adult. J Clin Endocrinol Metab 96(7):1966–1970. https://doi.org/10.1210/jc.2010-2104

Huang SA, Fish SA, Dorfman DM, Salvatore D, Kozakewich HP, Mandel SJ, Larsen PR (2002) A 21-year-old woman with consumptive hypothyroidism due to a vascular tumor expressing type 3 iodothyronine deiodinase. J Clin Endocrinol Metab 87(10):4457–4461. https://doi.org/10.1210/jc.2002-020627

Ito K, Uchida Y, Ohtsuki S, Aizawa S, Kawakami H, Katsukura Y, Kamiie J, Terasaki T (2011) Quantitative membrane protein expression at the bloodbrain barrier of adult and younger cynomolgus monkeys. J Pharm Sci 100(9):3939–3950. https://doi.org/10.1002/jps.22487

Kallo I, Mohacsik P, Vida B, Zeold A, Bardoczi Z, Zavacki AM, Farkas E, Kadar A, Hrabovszky E, Arrojo EDR, Dong L, Barna L, Palkovits M, Borsay BA, Herczeg L, Lechan RM, Bianco AC, Liposits Z, Fekete C, Gereben B (2012) A novel pathway regulates thyroid hormone availability in rat and human hypothalamic neurosecretory neurons. PLoS One 7(6):e37860. https://doi.org/10.1371/journal.pone.0037860

Karmarkar MG, Prabarkaran D, Godbole MM (1993) 5′-Monodeiodinase activity in developing human cerebral cortex. Am J Clin Nutr 57(2 Suppl):291S–294S

Kester MH, Martinez de Mena R, Obregon MJ, Marinkovic D, Howatson A, Visser TJ, Hume R, Morreale de Escobar G (2004) Iodothyronine levels in the human developing brain: major regulatory roles of iodothyronine deiodinases in different areas. J Clin Endocrinol Metab 89(7):3117–3128. https://doi.org/10.1210/jc.2003-031832

Larsen PR, Silva JE, Kaplan MM (1981) Relationships between circulating and intracellular thyroid hormones: physiological and clinical implications. Endocr Rev 2(1):87–102. https://doi.org/10.1210/edrv-2-1-87

Lavado-Autric R, Auso E, Garcia-Velasco JV, Arufe Mdel C, Escobar del Rey F, Berbel P, Morreale de Escobar G (2003) Early maternal hypothyroxinemia alters histogenesis and cerebral cortex cytoarchitecture of the progeny. J Clin Investig 111(7):1073–1082. https://doi.org/10.1172/JCI16262

López-Espíndola D, Morales-Bastos C, Grijota-Martínez C, Liao XH, Lev D, Sugo E, Verge CF, Refetoff S, Bernal J, Guadaño-Ferraz A (2014) Mutations of the thyroid hormone transporter MCT8 cause prenatal brain damage and persistent hypomyelination. J Clin Endocrinol Metab 99(12):E2799–E2804. https://doi.org/10.1210/jc.2014-2162

Marín-Padilla M (2015) Human cerebral cortex Cajal-Retzius neuron: development, structure and function. A Golgi study. Front Neuroanat 9:21. https://doi.org/10.3389/fnana.2015.00021

Martinez-Galan JR, Pedraza P, Santacana M, Escobar del Ray F, Morreale de Escobar G, Ruiz-Marcos A (1997) Early effects of iodine deficiency on radial glial cells of the hippocampus of the rat fetus. A model of neurological cretinism. J Clin Invest 99(11):2701–2709. https://doi.org/10.1172/jci119459

Matheus MG, Lehman RK, Bonilha L, Holden KR (2015) Redefining the pediatric phenotype of X-linked monocarboxylate transporter 8 (mct8) deficiency: implications for diagnosis and therapies. J Child Neurol. https://doi.org/10.1177/0883073815578524

Mayerl S, Muller J, Bauer R, Richert S, Kassmann CM, Darras VM, Buder K, Boelen A, Visser TJ, Heuer H (2014) Transporters MCT8 and OATP1C1 maintain murine brain thyroid hormone homeostasis. J Clin Investig 124(5):1987–1999. https://doi.org/10.1172/JCI70324

Mohan V, Sinha RA, Pathak A, Rastogi L, Kumar P, Pal A, Godbole MM (2012) Maternal thyroid hormone deficiency affects the fetal neocorticogenesis by reducing the proliferating pool, rate of neurogenesis and indirect neurogenesis. Exp Neurol 237(2):477–488. https://doi.org/10.1016/j.expneurol.2012.07.019

Mollgard K, Saunders NR (1986) The development of the human blood–brain and blood–CSF barriers. Neuropathol Appl Neurobiol 12(4):337–358

Morreale de Escobar G, Obregon MJ, del Rey FE (2004) Maternal thyroid hormones early in pregnancy and fetal brain development. Best Pract Res Clin Endocrinol Metab 18(2):225–248. https://doi.org/10.1016/j.beem.2004.03.012

Morte B, Bernal J (2014) Thyroid hormone action: astrocyte–neuron communication. Front Endocrinol 5:82. https://doi.org/10.3389/fendo.2014.00082

Nicholson JL, Altman J (1972) The effects of early hypo- and hyperthyroidism on the development of the rat cerebellar cortex. II. Synaptogenesis in the molecular layer. Brain Res 44(1):25–36

Oliveros JC (2007–2015) Venny. An interactive tool for comparing lists with Venn's diagrams. http://bioinfogp.cnb.csic.es/tools/venny/index.html

Pathak A, Sinha RA, Mohan V, Mitra K, Godbole MM (2011) Maternal thyroid hormone before the onset of fetal thyroid function regulates reelin and downstream signaling cascade affecting neocortical neuronal migration. Cereb Cortex 21(1):11–21. https://doi.org/10.1093/cercor/bhq052

Pollen AA, Nowakowski TJ, Chen J, Retallack H, Sandoval-Espinosa C, Nicholas CR, Shuga J, Liu SJ, Oldham MC, Diaz A, Lim DA, Leyrat AA, West JA, Kriegstein AR (2015) Molecular identity of human outer radial glia during cortical development. Cell 163(1):55–67. https://doi.org/10.1016/j.cell.2015.09.004

Roberts LM, Woodford K, Zhou M, Black DS, Haggerty JE, Tate EH, Grindstaff KK, Mengesha W, Raman C, Zerangue N (2008) Expression of the thyroid hormone transporters monocarboxylate transporter-8 (SLC16A2) and organic ion transporter-14 (SLCO1C1) at the blood–brain barrier. Endocrinology 149(12):6251–6261. https://doi.org/10.1210/en.2008-0378

Saunders NR, Habgood MD, Dziegielewska KM (1999) Barrier mechanisms in the brain, II. Immature brain. Clin Exp Pharmacol Physiol 26(2):85–91

Saunders NR, Dziegielewska KM, Mollgard K, Habgood MD (2018) Physiology and molecular biology of barrier mechanisms in the fetal and neonatal brain. J Physiol 596(23):5723–5756. https://doi.org/10.1113/JP275376

Schwartz CE, May MM, Carpenter NJ, Rogers RC, Martin J, Bialer MG, Ward J, Sanabria J, Marsa S, Lewis JA, Echeverri R, Lubs HA, Voeller K, Simensen RJ, Stevenson RE (2005) Allan–Herndon–Dudley syndrome and the monocarboxylate transporter 8 (MCT8) gene. Am J Hum Genet 77(1):41–53. https://doi.org/10.1086/431313

Sidman RL, Rakic P (1973) Neuronal migration, with special reference to developing human brain: a review. Brain Res 62(1):1–35

Siegenthaler JA, Ashique AM, Zarbalis K, Patterson KP, Hecht JH, Kane MA, Folias AE, Choe Y, May SR, Kume T, Napoli JL, Peterson AS, Pleasure SJ (2009) Retinoic acid from the meninges regulates cortical neuron generation. Cell 139(3):597–609. https://doi.org/10.1016/j.cell.2009.10.004

Smith D, Wagner E, Koul O, McCaffery P, Drager UC (2001) Retinoic acid synthesis for the developing telencephalon. Cereb Cortex 11(10):894–905

Stenzel D, Wilsch-Brauninger M, Wong FK, Heuer H, Huttner WB (2014) Integrin alphavbeta3 and thyroid hormones promote expansion of progenitors in embryonic neocortex. Development 141(4):795–806. https://doi.org/10.1242/dev.101907

Trajkovic M, Visser TJ, Mittag J, Horn S, Lukas J, Darras VM, Raivich G, Bauer K, Heuer H (2007) Abnormal thyroid hormone metabolism in mice lacking the monocarboxylate transporter 8. J Clin Investig 117(3):627–635. https://doi.org/10.1172/JCI28253

Van Herck SL, Delbaere J, Bourgeois NM, McAllan BM, Richardson SJ, Darras VM (2015) Expression of thyroid hormone transporters and deiodinases at the brain barriers in the embryonic chicken: insights into the regulation of thyroid hormone availability during neurodevelopment. Gen Comp Endocrinol 214:30–39. https://doi.org/10.1016/j.ygcen.2015.02.021

Vancamp P, Deprez MA, Remmerie M, Darras VM (2017) Deficiency of the thyroid hormone transporter monocarboxylate transporter 8 in neural progenitors impairs cellular processes crucial for early corticogenesis. J Neurosci 37(48):11616–11631. https://doi.org/10.1523/JNEUROSCI.1917-17.2017

Vatine GD, Al-Ahmad A, Barriga BK, Svendsen S, Salim A, Garcia L, Garcia VJ, Ho R, Yucer N, Qian T, Lim RG, Wu J, Thompson LM, Spivia WR, Chen Z, Van Eyk J, Palecek SP, Refetoff S, Shusta EV, Svendsen CN (2017) Modeling psychomotor retardation using ipscs from mct8-deficient patients indicates a prominent role for the blood–brain barrier. Cell Stem Cell 20(6):831–843. https://doi.org/10.1016/j.stem.2017.04.002

Westholm DE, Salo DR, Viken KJ, Rumbley JN, Anderson GW (2009) The blood–brain barrier thyroxine transporter organic anion-transporting polypeptide 1c1 displays atypical transport kinetics. Endocrinology 150(11):5153–5162. https://doi.org/10.1210/en.2009-0769

Whish S, Dziegielewska KM, Mollgard K, Noor NM, Liddelow SA, Habgood MD, Richardson SJ, Saunders NR (2015) The inner CSF–brain barrier: developmentally controlled access to the brain via intercellular junctions. Front Neurosci 9:16. https://doi.org/10.3389/fnins.2015.00016

Wirth EK, Roth S, Blechschmidt C, Holter SM, Becker L, Racz I, Zimmer A, Klopstock T, Gailus-Durner V, Fuchs H, Wurst W, Naumann T, Brauer A, de Angelis MH, Kohrle J, Gruters A, Schweizer U (2009) Neuronal 3′,3,5-triiodo-L-thyronine (T3) uptake and behavioral phenotype of mice deficient in Mct8, the neuronal T3 transporter mutated in Allan–Herndon–Dudley syndrome. J Neurosci 29(30):9439–9449. https://doi.org/10.1523/JNEUROSCI.6055-08.2009

Wirth EK, Sheu SY, Chiu-Ugalde J, Sapin R, Klein MO, Mossbrugger I, Quintanilla-Martinez L, de Angelis MH, Krude H, Riebel T, Rothe K, Kohrle J, Schmid KW, Schweizer U, Gruters A (2011) Monocarboxylate transporter 8 deficiency: altered thyroid morphology and persistent high triiodothyronine/thyroxine ratio after thyroidectomy. Eur J Endocrinol 165(4):555–561. https://doi.org/10.1530/EJE-11-0369

Yamaguchi S, Aoki N, Kitajima T, Iikubo E, Katagiri S, Matsushima T, Homma KJ (2012) Thyroid hormone determines the start of the sensitive period of imprinting and primes later learning. Nat Commun 3:1081. https://doi.org/10.1038/ncomms2088